Abelian dominance of chiral symmetry breaking in lattice QCD

Frank X. Lee and R.M. Woloshyn
TRIUMF, 4004 Wesbrook Mall, Vancouver, British Columbia, Canada V6T 2A3

Howard D. Trottier
Department of Physics, Simon Fraser University, Burnaby, British Columbia, Canada V5A 1S6
(Received 13 September 1995)

Calculations of the chiral condensate $\langle\bar{\chi}\chi\rangle$ on the lattice using staggered fermions and the Lanczos algorithm are presented. Four gauge fields are considered: the quenched non-Abelian field, an Abelian-projected field, and monopole and photon fields further decomposed from the Abelian field. Abelian projection is performed in the maximal Abelian gauge and in the Polyakov gauge. The results show that monopoles in the maximal Abelian gauge largely reproduce the chiral condensate values of the full non-Abelian theory, in both SU(2) and SU(3) color.

PACS number(s): 11.15.Ha, 11.30.Rd

I. INTRODUCTION

Since the Abelian monopole mechanism for confinement in QCD was first proposed [1,2], there have been extensive studies in the pure gauge sector of lattice theories [3–9]. The effect of Abelian-projection in the quark sector was studied in [10], where chiral symmetry breaking and meson correlators were analyzed. Further studies of the role of Abelian monopoles in chiral symmetry breaking at finite temperature [11], and in hadron spectroscopy [12], have been made. These works have provided evidence in support of Abelian monopoles as the mechanism of chiral symmetry breaking in QCD.

In the present work, a systematic study of the role of Abelian projection and monopoles in chiral symmetry breaking is carried out in the confined phase at zero temperature. The chiral condensate is computed using four sets of gauge fields: the quenched non-Abelian field, an Abelian projected field, and monopole and photon fields further decomposed from the Abelian projected field. Abelian projection is performed in the maximal Abelian gauge and in the Polyakov gauge. We employ a different technique to compute the chiral condensate than was used in Ref. [10], where an extrapolation to the chiral limit was made from nonzero quark mass: Here we use the spectral representation of the chiral condensate along with the Lanczos algorithm [13], which allows calculations to be done directly at zero mass. Most of the results presented here are for SU(2) color. Some results of a first study of chiral symmetry breaking in the Abelian projection of SU(3) gauge theory are also given.

The calculational method is described in Sec. II and results are presented in Sec. III. Using the Lanczos method at zero quark mass we find reasonable quantitative agreement between the chiral condensate calculated with the monopole part of the Abelian projected field and the quenched non-Abelian field for the SU(2) theory. Our present SU(3) simulation is not yet good enough to draw the same quantitative conclusion, but qualitatively, the same pattern emerges as seen in the SU(2) calculation. This provides some evidence that the Abelian dominance idea can be extended to the SU(3) theory.

Some of our results were presented in summary form in Ref. [14].

II. METHOD

A. Chiral condensate on the lattice

Chiral symmetry breaking is studied using staggered fermions, with the action

$$S_f = \frac{1}{2}\sum_{x,\mu}\eta_\mu(x)\Big[\bar{\chi}(x)\,U_\mu(x)\,\chi(x+\hat{\mu}) - \bar{\chi}(x+\hat{\mu})U_\mu^\dagger(x)\,\chi(x)\Big] + \sum_x m\bar{\chi}(x)\chi(x) \equiv \bar{\chi}\,\mathcal{M}(\{U\})\,\chi, \tag{1}$$

where $\bar{\chi},\chi$ are single-component fermion fields, $\eta_\mu(x)$ is the staggered fermion phase [15], m is the mass in lattice units, and the U's are gauge field links.

The chiral symmetry order parameter is calculated from the inverse of the fermion matrix $\mathcal{M}$ of Eq. (1):

$$\langle\bar{\chi}\chi(m,V)\rangle = \frac{1}{V}\langle\mathrm{Tr}\,\mathcal{M}^{-1}(\{U\})\rangle, \tag{2}$$

where V is the lattice volume and the angular brackets denote the gauge field configuration average. This can be rewritten in a spectral representation [16]

$$\langle\bar{\chi}\chi(m,V)\rangle = \frac{-1}{V}\sum_{n=1}^{N}\frac{1}{i\lambda_n+m} = \frac{-1}{V}\sum_{\lambda_n\geq 0}\frac{2m}{\lambda_n^2+m^2}, \tag{3}$$

where $i\lambda_n$'s are the eigenvalues of the zero-mass fermion matrix (Dirac operator). The eigenvalues appear in complex conjugate pairs, and so only the positive half of the

spectrum needs to be considered as in the second part of Eq. (3).

To correctly probe the physics of spontaneous chiral symmetry breaking, one should attempt to work in the limit of zero quark mass and infinite volume. The chiral limit $m \to 0$ should be taken after $V \to \infty$:

$$\langle \bar{\chi}\chi \rangle = -\lim_{m\to 0}\lim_{V\to\infty}\frac{1}{V}\sum_{\lambda_n \geq 0}\frac{2m}{\lambda_n^2 + m^2} = -\lim_{m\to 0}\int_0^\infty d\lambda \frac{2m\rho(\lambda)}{\lambda^2+m^2} = -\pi\rho(0), \quad (4)$$

where the spectral density function $\rho(\lambda) = \frac{1}{V}dn/d\lambda$ is normalized to $\int_0^\infty d\lambda\rho(\lambda) = N_c$, the number of colors. Equation (4) relates chiral symmetry breaking to the small modes in the eigenvalue spectrum. So the task is reduced to finding the small eigenvalues of the fermion matrix at zero mass, rather than the entire spectrum. This can be done using the well-established Lanczos algorithm [13].

B. Abelian projection on the lattice

The lattice formulation of Abelian projection was developed in [4,5]. The idea is to fix the gauge of a SU(N) theory so that a residual $U(1)^{N-1}$ gauge symmetry remains. The Abelian degrees of freedom are extracted by a subsequent projection $U(x,\mu) = c(x,\mu)u(x,\mu)$, where $u(x,\mu)$ is the (diagonal) Abelian-projected field and $c(x,\mu)$ the nondiagonal matter field. In general the gauge condition can be realized by diagonalizing some adjoint operator $\mathcal{R}$:

$$G(x)\mathcal{R}(x)G^{-1}(x) = \text{diagonal}. \quad (5)$$

Several gauge conditions have been studied and it has been found that the so-called maximal Abelian gauge [5] most readily captures the long-distance features of confinement (the relevance of other gauges to long-distance physics has been considered in [9]). In SU(2) this gauge is realized by maximizing the quantity

$$R = \sum_{x,\mu}\mathrm{tr}\left[\sigma_3\tilde{U}(x,\mu)\sigma_3\tilde{U}^\dagger(x,\mu)\right], \quad (6)$$

where $\tilde{U}(x,\mu) = G(x)U(x,\mu)G^{-1}(x+\mu)$. We maximize R by an iterative procedure. We find a gauge transformation $G(x)$ that maximizes R locally, at given site x, by keeping $G(x+\mu)$ at neighboring sites fixed. Using the fact $\sigma_3 G = G^\dagger\sigma_3$ (with the exception of diagonal gauge transformations) leads to an analytical solution for the local maximization of R:

$$G^2(x) = F^{-1}(x), \quad (7)$$

where

$$F(x) = \sum_{\mu=1}^{4}\Big[U(x,\mu)\sigma_3 U^\dagger(x,\mu)\sigma_3 + U^\dagger(x-\mu,\mu)\sigma_3 U(x-\mu,\mu)\sigma_3\Big]. \quad (8)$$

The global maximum of R is approached iteratively by repeatedly sweeping through the lattice, until $G(x)$ is sufficiently close to the identity

$$\max\left\{1 - \frac{1}{2}\mathrm{Tr}G(x)\right\} \leq \delta \ll 1, \quad \delta \sim 10^{-6}. \quad (9)$$

Maximal Abelian gauge in SU(3) is implemented by maximizing

$$R = \sum_{x,\mu}\left[|\tilde{U}_{11}(x,\mu)|^2 + |\tilde{U}_{22}(x,\mu)|^2 + |\tilde{U}_{33}(x,\mu)|^2\right]. \quad (10)$$

The maximization is done by going through the three SU(2) subgroups of SU(3). The gauge transformation within the first subgroup can be parametrized as

$$G_1(x) = \begin{pmatrix} g_0 & g_2 + ig_1 & 0 \\ -g_2 + ig_1 & g_0 & 0 \\ 0 & 0 & 1 \end{pmatrix}, \quad (11)$$

with the constraint $g_0^2 + g_1^2 + g_2^2 = 1$. R is maximized locally at x, again by holding G_1 at neighboring sites fixed. Under this local transformation, R can be expressed as

$$R = \sum_x\left[c_1 g_0^2 + c_2 g_1^2 + c_3 g_2^2 + c_4 g_0 g_1 + c_5 g_0 g_2\right], \quad (12)$$

where the sum over μ is implicit in the coefficients c_i. The solution is obtained numerically, and this is facilitated by introducing spherical coordinates on the unit sphere: $g_2 = \sin\theta\cos\phi$, $g_1 = \sin\theta\sin\phi$, $g_0 = \cos\theta$. This procedure is repeated at a given site for the second and the third subgroups. The global maximum of R is approached by repeatedly sweeping through the entire lattice until a stopping criterion similar to Eq. (9) is satisfied.

Once the gauge fixing is done, the Abelian-projected links are extracted. In SU(2) gauge theory, where the links can be parametrized by $\tilde{U}(x,\mu) = r_0 + i\vec{\sigma}\cdot\vec{r}$, the Abelian projected links u are given by

$$u = \mathrm{diag}(e^{i\phi}, e^{-i\phi}), \quad \phi = \arctan^{-1}(r_3/r_0). \quad (13)$$

In SU(3), the Abelian configurations are extracted according to

$$u = \mathrm{diag}(u_1,u_2,u_3), \quad u_k = \exp\left(i\arg\tilde{U}_{kk} - \frac{i}{3}\varphi\right), \quad (14)$$

where

$$\varphi = \left(\sum_k \arg\tilde{U}_{kk}\right) \mod 2\pi \subset (-\pi,\pi]. \quad (15)$$

The three phase factors are constrained by $u_1u_2u_3 = 1$ so that only two of them are independent.

C. Monopole decomposition

It is well known that there exist monopoles in a compact U(1) field. The Abelian-projected link $u(x,\mu) = \exp[i\phi_\mu(x)]$ can be resolved into a component due to monopoles by considering the Abelian field strength $\phi_{\mu\nu}(x)$, defined from plaquette phases in the usual way

$$\phi_{\mu\nu}(x) = \partial_\mu \phi_\nu(x) - \partial_\nu \phi_\mu(x), \tag{16}$$

where $\partial_\mu f(x) = f(x+\hat{\mu}) - f(x)$. The flux due to an integer-valued monopole string $\tilde{m}_{\mu\nu}$ is identified from the field strength according to [18]

$$\phi_{\mu\nu}(x) = \phi'_{\mu\nu}(x) + 2\pi\tilde{m}_{\mu\nu}(x), \tag{17}$$

where $\phi'_{\mu\nu} \in (-\pi,\pi]$. The vector potential $\phi^{\rm mon}_\mu(x)$ generated by the monopoles is therefore given (in Lorentz gauge) by

$$\phi^{\rm mon}_\nu(x) = -2\pi \sum_y D(x-y)\partial'_\mu \tilde{m}_{\mu\nu}(y), \tag{18}$$

where the lattice photon propagator satisfies $-\partial'_\mu\partial_\mu D(x) = \delta_{x,0}$, with $\partial'_\mu f(x) = f(x) - f(x-\hat{\mu})$ [17]. The "photon" field ϕ'_μ is identified with the difference $\phi_\mu(x) - \phi^{\rm mon}_\mu(x)$.

III. NUMERICAL RESULTS

The Lanczos algorithm [13] is carried out in double precision to find the eigenvalues of the fermion matrix. To test our implementation of the algorithm, the full spectra of an 8^4 lattice and a 12^4 lattice at β=2.3 in SU(2) were obtained for one configuration. In SU(2) one knows *a priori* that every eigenvalue is doubly degenerate so that the number of single positive eigenvalues must be $V/2$. Furthermore, they satisfy the closure relation $\sum_{n=1}^{V/2}\lambda_n^2 = V$. We found exactly 2048 single positive eigenvalues for the 8^4 lattice and 10 368 for the 12^4 lattice, and the closure relations were satisfied to a few parts in 10^8. This indicates that we can determine the spectrum accurately.

A. Results for SU(2)

A heat-bath Monte Carlo algorithm was used to generate quenched gauge field configurations using the standard Wilson plaquette action, with periodic boundary conditions on a 14^4 lattice at β=2.2, 2.3, 2.4, and 2.5. Antiperiodic boundary conditions were used for fermions in all directions. Other boundary conditions were also tried, and our results showed little change. Gauge fixing was done with the help of overrelaxation [19] which reduced the number of iterations by a factor of 3–5. About 500 iterations with overrelaxation were required for a stopping criterion $\delta \sim 10^{-6}$.

In Fig. 1 we show the raw data for the spectral density function $\rho(\lambda)$ obtained from 70 configurations at each β value. The results clearly show a nonvanishing signal of $\rho(\lambda)$ at all β values, although finite volume effects,

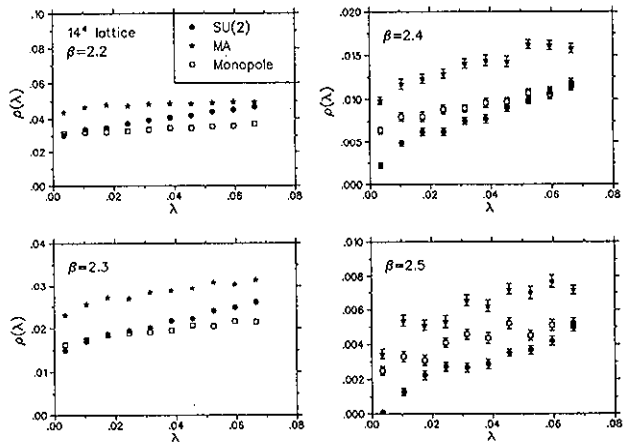

FIG. 1. Spectral density functions calculated at four different β values for three types of gauge configurations: the non-Abelian SU(2) configurations, the Abelian-projected configurations in the maximal Abelian gauge, and the monopole configurations further decomposed from the Abelian-projected configurations.

manifested as a sudden depletion near $\lambda = 0$ [20], begin to set in at β=2.4 and 2.5. To extract a value at $\lambda = 0$, we fit the distributions by a straight line $\rho(\lambda) = \rho(0) + \rho'(0)\lambda$ in an interval $[\lambda_{\rm min}, \lambda_{\rm max}]$. The interval is chosen so that it excludes those eigenvalues near $\lambda = 0$ that are strongly influenced by finite volume effects and those that cause $\rho(\lambda)$ to depart from linear behavior. It is expected that $\lambda_{\rm min} \sim \xi^3/V$ where ξ is some length scale governed by the gluon dynamics [20]. The value $\lambda_{\rm max}$ is chosen to be as large as possible while preserving both the stability and the quality of the fit. Under these conditions, we find that the fit is quite stable over a relatively wide interval. Figure 2 shows the results of such a fit for the eigenvalue interval [0.015,0.05]. The fitted values for $\rho(0)$ and $\rho'(0)$ and the extracted chiral condensate $\langle\bar{\chi}\chi\rangle$ are given in Table I in lattice units. The errors quoted are statistical and are obtained using the jackknife method. Since the eigenvalue spectrum is doubly degenerate, the quoted numbers for $\rho(\lambda)$ are only half of the true value,

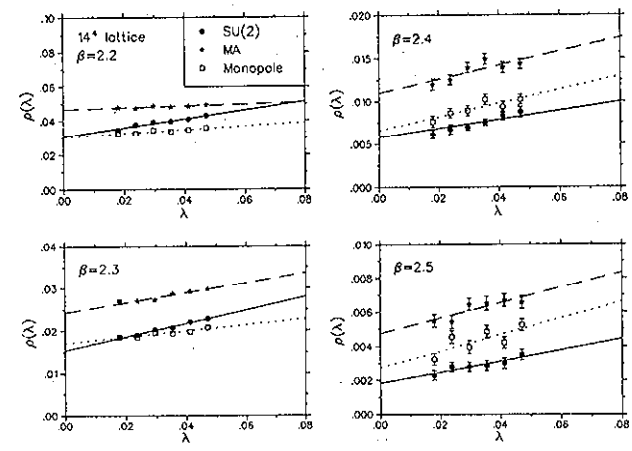

FIG. 2. Fitted spectral density functions in the interval [0.015,0.05] in SU(2).

TABLE I. The extracted values for $\langle\bar{\chi}\chi\rangle$ on the 14^4 lattice from the straight line fit $\rho(\lambda) = \rho(0) + \rho'(0)\lambda$ in the interval [0.015,0.05]. At each β value, the first row is for the full SU(2), second row maximal Abelian, third row monopole. Numbers in parentheses are statistical errors in the final digit(s).

β	$\rho(0)$	$\rho'(0)$	$-\langle\bar{\chi}\chi\rangle$
2.2	0.0307(4)	0.258(10)	0.193(2)
	0.0466(5)	0.052(14)	0.293(3)
	0.0303(5)	0.107(14)	0.190(3)
2.3	0.0154(4)	0.158(11)	0.097(3)
	0.0243(5)	0.116(13)	0.153(3)
	0.0170(5)	0.072(13)	0.107(3)
2.4	0.0058(6)	0.052(21)	0.036(4)
	0.0110(7)	0.080(19)	0.069(4)
	0.0066(7)	0.080(21)	0.041(5)
2.5	0.0018(3)	0.033(09)	0.011(2)
	0.0047(5)	0.045(13)	0.030(3)
	0.0028(4)	0.048(12)	0.017(3)

so that the extracted $\langle\bar{\chi}\chi\rangle = -2\pi\rho(0)$. The value of $\langle\bar{\chi}\chi\rangle$ in the full SU(2) theory and in the maximal Abelian gauge projection are consistent with those obtained in Ref. [10], where an extrapolation to the chiral limit was made from nonvanishing quark mass. The interesting feature here is that the monopole configuration average has a condensate that is even closer to the full theory than the Abelian projected fields. On the other hand with the photon configurations either no or very few small eigenvalues are found. Hence we conclude there is no chiral symmetry breaking from these configurations.

For purposes of comparison, we also performed Abelian projection at $\beta = 2.5$ using a different gauge-fixing condition: the Polyakov gauge, in which the Polyakov loop is diagonalized according to Eq. (5). The result is shown in Fig. 3. We see that the Abelian and the monopole field spectral density functions are almost an order of magnitude larger than those of the full theory. In Ref. [10], a similar result for $\langle\bar{\chi}\chi\rangle$ is found using the field-strength gauge.

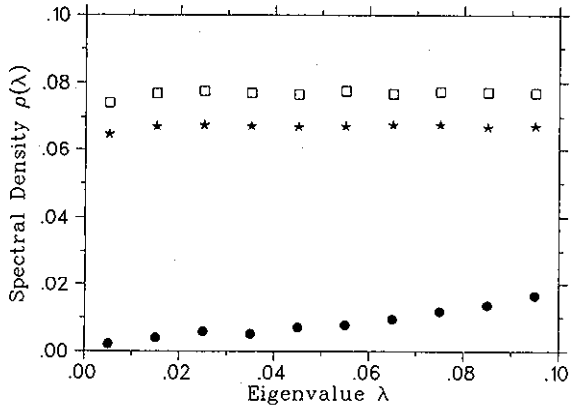

FIG. 3. Spectral density functions calculated in the Polyakov gauge at β=2.5 for three types of gauge configurations: non-Abelian SU(2)(•), Abelian(□), and monopole(⋆).

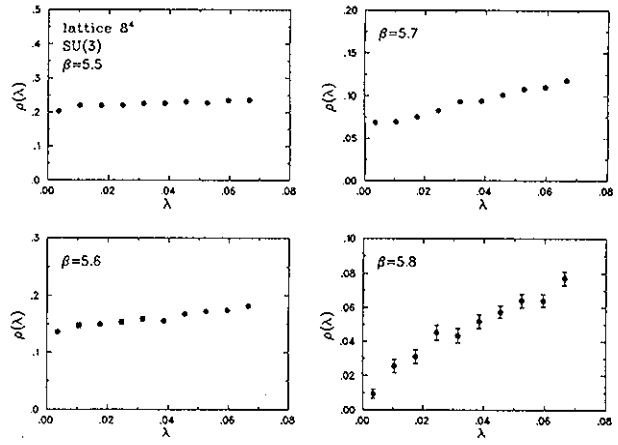

FIG. 4. Spectral density functions calculated at four different β values in SU(3).

B. Results for SU(3)

The gauge field configurations were generated using the Cabibbo-Marinari [20] pseudo-heat-bath method on a 8^4 lattice at β=5.5, 5.6, 5.7, 5.8, and 10^4 lattice at β = 5.9. Configurations are selected after 4000 thermalization sweeps from a cold start, and every 500 sweeps thereafter. Figure 4 shows the spectral density function obtained from 44 SU(3) gauge field configurations for β=5.5, 66 configurations for β=5.6, 150 configurations for β=5.7, and 37 configurations for β=5.8.

We performed Abelian projections on the 8^4 lattice at $\beta = 5.7$ and 10^4 lattice at $\beta = 5.9$. Gauge fixing in SU(3) is time consuming. On average about 500 iterations with overrelaxation are required for $\delta = 1 - \frac{1}{9}\mathrm{Tr}[G_1(x) + G_2(x) + G_3(x)]$ to converge to 10^{-5}. After configuration averaging, the three phase factors in Eq. (14) give equal contributions to the chiral condensate. So the total is obtained by first calculating with one phase and then multiplying by 3. This saves a factor of 3 in computer time. Figures 5 and 6 show the data obtained for $\rho(\lambda)$. For the 8^4 lattice at $\beta = 5.7$, 150 configurations were used, and 100 configurations for 10^4 at

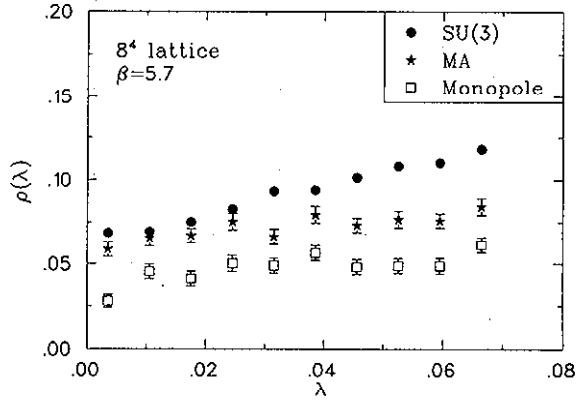

FIG. 5. Spectral density function in the SU(3) case on the 8^4 lattice at β=5.7.

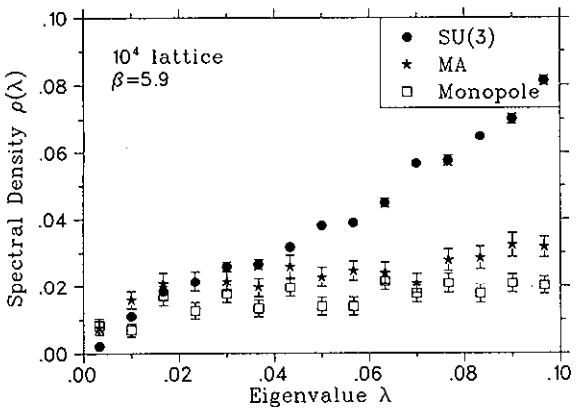

FIG. 6. Spectral density function in the SU(3) case on the 10^4 lattice at β=5.9.

$\beta = 5.9$. We see that a similar pattern emerges in SU(3) as in SU(2): For small eigenvalues, the Abelian and the monopole contributions give spectral densities that are close to those of the full theory. It was also confirmed that photon configurations give negligible contributions.

IV. CONCLUSION

We have calculated chiral symmetry breaking on the lattice in the quenched approximation and Abelian projection. Unlike the previous study [10], the Lanczos method is used to calculate eigenvalues of the fermion matrix and hence the chiral condensate directly at zero quark mass. Furthermore, in this work, a decomposition of the Abelian-projected field into monopole and photon pieces was made. For SU(2) gauge theory it was found the monopole part of the Abelian field, projected in the maximal Abelian gauge, yields chiral condensate values which are quite close to those obtained with the full non-Abelian fields. In contrast, the photon piece of the Abelian-projected field gives no condensate.

A calculation was also done using Abelian fields projected in the Polyakov gauge. This yielded an eigenvalue density and hence a chiral condensate about an order of magnitude larger than the non-Abelian calculation. This is consistent with what was previously found in field strength gauge in Ref. [10].

Some calculations were also done in an SU(3) theory. Qualitatively, a similar pattern is seen as in the SU(2) calculation. In the region of small eigenvalues (which is relevant for chiral symmetry breaking), the Abelian and monopole fields give spectral densities which are quite close to that of the full non-Abelian calculation. This provides a positive indication that the idea of Abelian dominance can be extended to the SU(3) theory.

ACKNOWLEDGMENT

This work was supported in part by the Natural Sciences and Engineering Council of Canada.

[1] G. 't Hooft, in *Proceedings of the EPS International Conference on High Energy Physics*, Palermo, 1975, edited by A. Zichichi (Editrice Compositori, Bologna, 1976); S. Mandelstam, Phys. Rep. **23C**, 245 (1976).
[2] G. 't Hooft, Nucl. Phys. **B190**, 455 (1981).
[3] T. Suzuki and I. Yotsuyanagi, Phys. Rev. D **42**, 4257 (1990); S. Hioki *et al.*, Phys. Lett. B **272**, 326 (1991).
[4] A. S. Kronfeld, G. Schierholz, and U.-J. Wiese, Nucl. Phys. **B293**, 461 (1987).
[5] A. S. Kronfeld, M. L. Laursen, G. Schierholz, and U.-J. Wiese, Phys. Lett. B **198**, 516 (1987).
[6] F. Brandstaeter, G. Schierholz, and U.-J. Wiese, Phys. Lett. B **272**, 319 (1991).
[7] L. Del Debbio, A. Di Giacomo, M. Maggiore, and S. Olejnik, Phys. Lett. B **267**, 254 (1991); A. Di Giacomo, Report No. hep-lat/9505006 (unpublished).
[8] K. Yee, Phys. Rev. D **49**, 2574 (1994).
[9] G. I. Poulis, H. D. Trottier, and R. M. Woloshyn, Phys. Rev. D **51**, 2398 (1995).
[10] R. M. Woloshyn, Phys. Rev. D **51**, 6411 (1995).
[11] O. Miyamura, in *Lattice '94*, Proceedings of the International Symposium, Bielefeld, Germany, edited by F. Karsch *et al.* [Nucl. Phys. B (Proc. Suppl.) **42**, 538 (1995)].
[12] T. Suzuki *et al.*, in *Lattice '95*, Proceedings of the International Symposium, Melbourne, Austria [Nucl. Phys. B (Proc. Suppl.) (in press)].
[13] See, for example, J. K. Cullum and R. A. Willoughby, *Lanczos Algorithms for Large Symmetric Eigenvalue Computations* (Birkhäuser, Boston, 1985); G. H. Golub and C. F. van Loan, *Matrix Computations*, 2nd ed. (The John Hopkins University Press, Baltimore, 1990).
[14] F. X. Lee, R. M. Woloshyn, and H. D. Trottier, *Lattice '95* [12].
[15] N. Kawamoto and J. Smit, Nucl. Phys. **B192**, 100 (1981).
[16] I. M. Barbour, P. Gibbs, K. C. Bowler, and D. Roweth, Phys. Lett. **158B**, 61 (1985).
[17] T. A. DeGrand and D. Toussaint, Phys. Rev. D **22**, 2478 (1980).
[18] J. Smit and A. J. van der Sijs, Nucl. Phys. **B355**, 603 (1991).
[19] J. E. Mandula and M. Ogilvie, Phys. Lett. B **248**, 156 (1990).
[20] For a detailed discussion of these effects, see S. J. Hands and M. Teper, Nucl. Phys. **B347**, 819 (1990).
[21] N. Cabibbo and E. Marinari, Phys. Rev. Lett. **119B**, 387 (1982).